



OPEN ACCESS

EDITED BY

Antoinette Van Der Kuyl,
University of Amsterdam, Netherlands

REVIEWED BY

Assunta Venuti,
International Agency for Research on
Cancer (IARC), France
Adriana Aguilar Lemarroy,
Centro de Investigación Biomédica
de Occidente (CIBO), Mexico

*CORRESPONDENCE

Qingling Ren
yfy0047@njucm.edu.cn

SPECIALTY SECTION

This article was submitted to
Virology,
a section of the journal
Frontiers in Microbiology

RECEIVED 27 June 2022

ACCEPTED 16 August 2022

PUBLISHED 14 September 2022

CITATION

Dai R, Tao R, Li X, Shang T, Zhao S and
Ren Q (2022) Expression profiling
of mRNA and functional network
analyses of genes regulated by human
papilloma virus E6 and E7 proteins
in HaCaT cells.

Front. Microbiol. 13:979087.

doi: 10.3389/fmicb.2022.979087

COPYRIGHT

© 2022 Dai, Tao, Li, Shang, Zhao and
Ren. This is an open-access article
distributed under the terms of the
[Creative Commons Attribution License
\(CC BY\)](https://creativecommons.org/licenses/by/4.0/). The use, distribution or
reproduction in other forums is
permitted, provided the original
author(s) and the copyright owner(s)
are credited and that the original
publication in this journal is cited, in
accordance with accepted academic
practice. No use, distribution or
reproduction is permitted which does
not comply with these terms.

Expression profiling of mRNA and functional network analyses of genes regulated by human papilloma virus E6 and E7 proteins in HaCaT cells

Renjinming Dai¹, Ran Tao², Xiu Li¹, Tingting Shang¹,
Shixian Zhao¹ and Qingling Ren^{1*}

¹The Affiliated Hospital of Nanjing University of Chinese Medicine, Nanjing, China, ²Laboratory of Clinical Applied Anatomy, Department of Human Anatomy, School of Basic Medical Sciences, Fujian Medical University, Fuzhou, China

Human papillomavirus (HPV) oncogenes E6 and E7 are essential for HPV-related cancer development. Here, we developed a cell line model using lentiviruses for transfection of the HPV16 oncogenes E6 and E7 and investigated the differences in mRNA expression during cell adhesion and chemokine secretion. Subsequently, RNA sequencing (RNA-seq) analysis was performed to explore the differences in mRNA expression. Compared to levels in the control group, 2,905 differentially expressed mRNAs (1,261 downregulated and 1,644 upregulated) were identified in the HaCaT-HPV16E6E7 cell line. To predict the functions of these differentially expressed genes (DEGs) the Gene Ontology and Kyoto Encyclopedia of Genes and Genomes databases were used. Protein-protein interactions were established, and the hub gene was identified based on this network. Real-time quantitative-PCR (RT-qPCR) was conducted to confirm the levels of 14 hub genes, which were consistent with the RNA-seq data. According to this, we found that these DEGs participate in the extracellular matrix (ECM), cell adhesion, immune control, and cancer-related signaling pathways. Currently, an increasing number of clinicians depend on E6/E7mRNA results to make a comprehensive judgment of cervical precancerous lesions. In this study, 14 hub genes closely related to the expression of cell adhesion ability and chemokines were analyzed in HPV16E6E7-stably expressing cell lines, which will open up new research ideas for targeting E6E7 in the treatment of HPV-related cancers.

KEYWORDS

cell adhesion, cervical epithelioma, differentially expressed genes, HPV, oncogenes, RNA sequencing

Introduction

The human papillomavirus (HPV) is a DNA virus that encodes approximately eight genes. It can cause cancers of the antrum, genital tract, upper respiratory tract, and digestive tract (Dunne and Park, 2013). High-risk HPV E6 and E7 proteins reduce immune recognition by disrupting cell adhesion, polarity, and transcription via several pathways, such as the cell adhesion pathway (Oldak et al., 2006; Whiteside et al., 2008; Howie et al., 2009; Läubli and Borsig, 2019; Kombe Kombe et al., 2020). Studies have shown that the cervical squamous epithelium, which is the target of HPV, consists of keratinocytes, immature dendritic cells (DCs), and Langerhans cells (LCs), all of which perform immunosurveillance functions on the epithelium (Schiffman et al., 2007). LCs are the only specialized antigen-presenting cells found in the epidermis, and their abnormal expression affects antiviral immune responses. HPV-associated cervical squamous epithelial neoplasia (SIL) is strongly associated with immature LCs (Habbous et al., 2012). Cell adhesion between cells and the extracellular matrix (ECM) is required for the integrity of the epidermis and the formation of an immune barrier (Honig and Shapiro, 2020). Cell surface adhesion molecules, the major components of cell-to-cell and cell-to-extracellular interactions (Login et al., 2019), are frequently expressed in epithelial (Sumigray and Lechler, 2015), endothelial (Schimmel and Gordon, 2018), and immune (Dustin, 2009) cells. They consist of intracellular and extracellular components (CC) and can be divided into four types, cadherins, integrins, selectins, and immunoglobulins. Many studies have focused on malignant metastasis and cell adhesion (Janiszewska et al., 2020); however, the mechanisms related to interactions among HPV proteins, cell adhesion, and the epithelial immune response remains unclear. Activated leukocyte cell adhesion molecule (ALCAM) (Ferragut et al., 2021) is a cell-surface glycoprotein that has been recognized as a vital prognostic marker for various tumors, including HPV-associated head and neck squamous cell carcinoma (Zhu et al., 2020). Based on current research, ALCAM can regulate adhesion to immune cells (Te Riet et al., 2014) and control disease progression by affecting cell proliferation, migration, and invasion (von Lersner et al., 2019).

Chemokines are the largest subfamily of cytokines (Bule et al., 2021). It is well known that HPV is capable of preventing a robust immune response to the infected cells based on many mechanisms, such as by reducing the expression of chemokines (Attademo et al., 2020; Acevedo-Sánchez et al., 2021). When chemokines are unable to guide immune cells to migrate to the infected site in an orderly fashion, immune tolerance collapses and immune monitoring becomes ineffective (Kolaczowska and Kubes, 2013).

With the increasing prevalence of Illumina technology in recent years, RNA-sequencing (RNA-Seq) technology has been effectively used in biomedical research (Tao et al., 2021; Wang

et al., 2021). The carcinogenetic effect of E6 and E7 is apparent, but molecules that are induced by these proteins in HaCaT cells still need to be researched, and high-throughput sequencing would contribute vastly to this question. In this research, the differential mRNA expression profiles of HPV16E6E7-stably expressing cell lines were determined via RNA-seq. Our results showed that transcriptome levels were significantly different between the two groups of non-transfected control and HPV16E6E7-stably expressing cell lines. Transcriptome data are essential in providing a research target for mechanistic studies aimed at reversing cervical epithelioma and blocking the malignant progression of epithelial cells.

Materials and methods

Cell adhesion assays

E6-IRES-E7 was constructed and inserted into the plenti-Gm-cMV vector to obtain the vector plasmidpLenti-III-HPV-16E6-IRES-E7Vector (Puro). It was co-transfected with Lenti-ComboPackingMix and lentifectin into HEK293T. Cell supernatants were collected after the transfection, and the lentivirus was designated as Lenti-III-HPV-16E6-IRES-E7Virus (Puro). HaCaT cells were seeded onto 6-well plates at a density of approximately 20–30%, and then were infected with the lentivirus and incubated at 5% CO₂, 37°C for 48 h. The infected HaCaT cells were plated in 96-well plates for stable transfection strain resistance screening. After HaCaT in logarithmic growth phase was infected by Lenti-III-HPV-16 E6-IRES-E7 Virus (Puro), four monoclonal cell lines, clone#4, clone#6, clone#10, clone#11, were obtained. Clone#11 showed the highest expression of target gene, validated by Real-time quantitative-PCR (RT-qPCR). Our team collaborated with ABM (Applied Biological Materials, Jiangsu, China) to establish this HaCaT-HPV16E6/E7. According to the introduction of the commercial cell adhesion kit (BestBio, Shanghai, China), the adhesion ability of parental HaCaT and HaCaT-HPV16E6E7 cells was defined. The optical density was recorded at 450 nm using a microplate reader (TECAN, SCHWEIZ). Finally, the level of cell adhesion was analyzed based on the OD value.

Western blot analysis

Protein samples were extracted from parental HaCaT and HaCaT-HPV16E6/E7 Clone#11 cell which were harvested in three different generations using RIPA buffer (Beyotime Biotechnology, Shanghai, China). Determination of total protein was performed using a commercial kit (Beyotime Biotechnology, Shanghai, China), and then, samples were incubated at 100°C for 10 min. Protein samples were separated

with 2–8% precast gels (ACE Biotechnology, Nanjing, China) and transferred onto PVDF (Millipore, Massachusetts, United States). The membranes were then soaked with 5% skim milk at 20–22°C for 1 h. After this, the solution was removed, and the membranes were incubated with primary antibodies, including those against ALCAM (1:1,000, Abmart, T57159), HPV16 E7 (1:500, bs-4623R), and HPV16 E6 (1:500, Abmart, V028329). The following day, the membrane was incubated with the secondary antibody (1:5,000, Cell Signaling Technology, 7076/7074) at 20–22°C for 1 h. The protein bands were developed using an ultrasensitive luminescent liquid reagent (Tanon, Shanghai, China) and analyzed using Image Lab version 5.1. The band density of the target protein to that of β -actin was used as the relative target protein content. All western blot experiments consisted of at least 3 independent replicates.

Real-time quantitative-PCR

We examined expression levels of the chemokine genes *CCL2*, *CCL3*, *CCL5*, *CCL7*, and *CXCL10* using RT-qPCR. The mRNA levels were determined by real time PCR. Total RNA was extracted from the parental HaCaT and HaCaT-HPV16E6/E7 Clone#11 cell which were harvested in three different generations using an RNA extraction kit (Vazyme, Nanjing, China). The cDNA product was obtained via reverse transcription using a commercial reagent at 37°C for 15 min and then 85°C for 5 s (Vazyme, Nanjing, China). GAPDH and β -actin were used as internal controls. Primers were pre-designed and synthesized from a company (Sangon Biotech, Shanghai, China), and primer sequences are described in [Table 1](#). Products were amplified using QUANTSTUDIO 7 FLEX QUANTSTUDIO (ABAppliedBiosystems, United States) according to the instructions for the Taq Pro Universal SYBR qPCR Master Mix kit (Vazyme, Nanjing, China). RT-qPCR was performed in technical triplicate for each biological replicate. Finally, Real-time PCR results were calculated according to the $\Delta\Delta$ CT method by using GAPDH and β -ACTIN as housekeeping genes.

RNA-Seq and gene expression analysis

RNA samples harvested from the parental HaCaT and HaCaT-HPV16E6/E7 Clone#11 cell, which were harvested in four different generations and were used for sequencing. Libraries for RNA-Seq were obtained from total RNA, and sequencing was performed on the NovaSeq 6000 platform by Gene *Denovo* Biotechnology Co., Ltd (Guangzhou, China). To quantify gene expression, HTSeq was used to obtain the original read count for each gene; alternatively, reads per kilobase of transcript per million mapped reads (RPKM) were used

depending on the total map read count and the gene length for each sample. DEGs were determined based on the gene expression level measured using \log_2 -transformed RPKM ($|\log_2FC|$ (fold change) > 2, FDR < 0.01). The read counts data were entered and analyzed using EdgeR and DESeq2 software, including normalization of read counts and calculation of *P*-values and FDR values. Transcriptome data (SRA accession: PRJNA850539) were stored in the NCBI SRA database.¹

Enrichment analysis

GO enrichment analysis includes biological process (BP), molecular function (MF), and CC, three aspects that are based on significantly enriched DEGs. The differential genes are mapped to each term of the GO database and the number of genes per term is counted to obtain a list of genes with a certain GO function and gene number statistics. Hypergeometric tests were applied to identify GO terms that were significantly enriched in differential genes compared to the whole genomic background. Briefly, all DEGs were mapped to GO terms in the GO database.² Then, gene numbers were calculated for every term, and GO terms associated with significantly enriched DEGs compared to the genome background were defined using a hypergeometric test. The calculated *p*-value was subjected to false discovery rate (FDR) correction, with $FDR \leq 0.05$ as the threshold. Pathways meeting this condition were defined as significantly enriched pathways among the DEGs. The KEGG analysis was carried out according to KEGG.³ GSEA was also performed with the GSEA software.⁴

Generation of the protein–protein interaction network

The protein–protein interaction (PPI) network was constructed using the String database,⁵ for which genes and interactions were determined and designated as nodes and lines, respectively, in the network. To show the biological interactions among DEGs, their relationship network was visualized using Cytoscape (v3.9.2) software. Moreover, the cytoHubba plug-in was used to mine the hub genes using the MNC, Stress, Degree, Closeness, and Radiality calculation method in the Cytoscape MCODE plug-in Cytoscape, which was used to further extract the core sub-networks.

1 <https://www.ncbi.nlm.nih.gov/bioproject/PRJNA850539>

2 <http://www.geneontology.org/>

3 <http://www.genome.jp/kegg/>

4 <http://www.broadinstitute.org/gsea>

5 <https://cn.string-db.org/>

TABLE 1 Primer lists.

Gene	Forward primer (5'-3')	Reverse primer (5'-3')
GAPDH	CATCATCCCTGCCTCTACTG	CTGCTTCACCACCTTCTTG
β -actin	GGCACCCAGCACAAATGAAG	CCGATCCACACGGAGTACTTG
CCL2	CAGCCAGATGCAATCAATGCC	TGGAATCCTGAACCCACTTCT
CCL5	CCAGCAGTCGTCTTTGTGAC	CTCTGGGTTGGCACACACTT
CCL7	GCCTCTGCAGCACTTCTGTG	CACTTCTTGTGTGGGGTCAGC
CXCL10	GTGGCATTCAAGGAGTACCTC	TGATGGCCTTCGATTCTGGATT
CCL3	CAGCCAGATGCAATCAATGCC	TGGAATCCTGAACCCACTTCT
CDH1	CGAGAGCTACACGTTACCGG	GGGTGTCGAGGGAAAAATAGG
CDH2	TCAGGCGTCTGTAGAGGCTT	ATGCACATCCTTCGATAAGACTG
EGF	TGGATGTGCTTGATAAGCGG	ACCATGTCCTTCCAGTGTGT
FGF2	AGAAGAGCGACCCTCACATCA	CGGTTAGCACACACTCCTTTG
BDNF	GGCTTGACATCATTTGGCTGAC	CATTGGGCCGAACTTCTGGT
SOX2	GCCGAGTGGAACTTTTGTGCG	GGCAGCGTGTACTTATCCTTCT
TLR4	AGACCTGTCCCTGAACCCTAT	CGATGGACTTCTAAACCAGCCA
IGF1	GCTCTTCAGTTCGTGTGTGGA	GCCTCCTTAGATCACAGCTCC
DLG4	TCGGTGACGACCATCCAT	GCACGTCCACTTCATTTACAAAC
COL1A1	GAGGGCCAAGACGAAGACATC	CAGATCACGTATCGCACAAAC
FYN	ATGGGCTGTGTGCAATGTAAG	GAAGCTGGGGTAGTGTCTGAG
CXCR4	ACTACACCGAGGAAATGGGCT	CCCACAATGCCAGTTAAGAAGA
WNT5A	ATTCTTGGTGGTCGCTAGGTA	CGCCTTCTCCGATGTACTGC
IL-1 β	TCGCCAGTGAATGATGGCT	TGGAAGGAGCACTTCATCTGTT

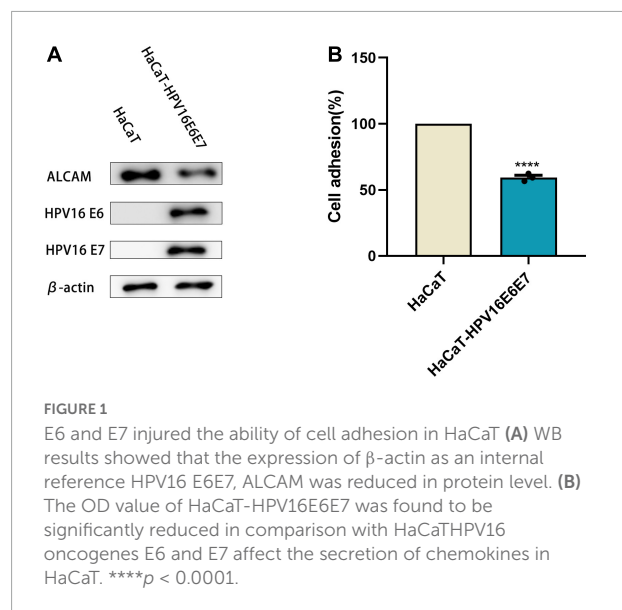
Statistical analysis

Data are presented from three independent experiments based on the means \pm SEMs. For statistical analyses, GraphPad Prism 9 software was adopted (GraphPad, United States). When comparing two groups, unpaired *t*-tests were used, and differences among groups were analyzed using one-way ANOVA. A *p*-value < 0.05 was considered statistically significant.

Results

Human papillomavirus 16 oncogenes E6 and E7 affect cell adhesion in HaCaT cells

HaCaT cells stably expressed the E6 and E7 proteins after lentiviral transduction (Supplementary Figure 1). A cell adhesion reagent kit was used to determine whether this inhibited cell adhesion by measuring the optical density value in each group of cells. The overexpression of E6 and E7 significantly reduced the cell absorbance, indicating that they negatively affected cell adhesion (Figure 1B). Simultaneously, the protein expression level of the cell adhesion molecule (CAM) ALCAM was significantly decreased when examined via western blotting analysis (Figure 1A and Supplementary Figures 2, 3).



Human papillomavirus16 oncogenes E6 and E7 affect HaCaT cell adhesion

Chemokines are effective chemical attractants for natural killer cells, macrophages, and monocytes, and they engage in the host immune response against HPV-infected cervical epithelia. CCL2, CCL3, CCL5, and CCL7 attract monocytes/macrophages

to exert anti-infective, anti-tumor, and immunomodulatory effects at sites of inflammation. In response to pro-inflammatory stimuli, such as IL-1, TNF- α , LPS, or viruses, the expression of CCL2, CCL3, CCL5, and CXCL10 recruit immune cells to sites of inflammation. However, after overexpression of the HPV E6/E7 protein, the expression levels of CCL2, CCL3, CCL5, CCL7, and CXCL10 decreased with different magnitudes. The selective loss of chemokine expression, including that of CCL2, was observed after lentiviral transduction. Moreover, their mRNA levels were significantly lower than those in keratinocyte HaCaT cells (Figure 2 and Supplementary Figure 4).

Overview of differential mRNA expression

The original RNA-seq data (Read Count) and differential expression analysis results (DESeq2_analysis_results) used in this study were uploaded, and these tables can be found in the Supplementary Material 1. To identify DEGs between the cell groups, the Limma package was used to analyze data. The criteria were as follows: $|\log_2FC| > 2$ and $p < 0.01$ (Figure 3A). After this step, the mRNA expression of 1,644 genes were found to be upregulated, whereas that of 1,261 genes was downregulated; according to our data, DEGs based on mRNA expression were presented as a volcano map using the ggplot2 package (Figure 3B). Heatmaps of the DEGs were created with the heatmap package (Figure 3C).

Enrichment analyses of differentially expressed mRNAs

The top 20 KEGG pathways (Figure 4A) indicated that DEGs were enriched in the Hippo and Wnt pathways and signaling pathways that regulate the ECM receptor interaction, among others. These signaling pathways exhibit crosstalk with cell adhesion by regulating the transcription of chemokines, CAMs, and growth factors, including cadherin 1 (CDH1), CDH2, epidermal growth factor (EGF), brain-derived neurotrophic factor (BDNF), interleukin (IL)-1 β , fibroblast growth factor (FGF2), disks large homolog 4 (DLG4), Toll-like receptor 4 (TLR4), insulin-like growth factor 1 (IGF1), collagen type I alpha 1 (COL1A1), CXCR4, and WNT5A. In the GO analysis, DEGs closely related to several BP, MF, and CC included genes involved in adhesion, immune system, cell aggregation, transcription regulator activity, and cell junction (Figure 4B). In addition, GESA and KEGG analyses showed similar results, such as genes involved in tight junctions (Supplementary Figure 5).

Analysis of protein–protein interaction network

To provide a better understanding of interactions among the DEGs, their corresponding PPI network was generated using Cytoscape software and the STRING database. The “cytoHubba” plug-in identified the 14 core genes based on differences in the level of linkage (Figures 5A–E). These 14 hub genes are obtained by taking the intersection of the DEGs obtained from five different algorithms, and are presented with the form of Venn diagram (Figure 5F). The interactive density region in the PPI network was also determined using the “MCODE” plug-in (Figures 6A–D). The figure below shows the densest regions (Figure 5E). For example, BDNF binds to CDH2 and CXCR4, TLR4 to CXCR4 and IL-1 β , and CDH1 to FYN and IGF1. In this study, it was considered that these proteins play useful roles in regulating chemokine binding and macrophage-mediated cytokine production.

Verification of differentially expressed mRNAs

RT-qPCR was performed to verify the transcriptome sequencing results before and after lentiviral transduction and define the possible signaling network associated with the E6 and E7 oncogenes upon HPV16 infection. The RT-qPCR data showed that the expression of CXCR4 was decreased in cells overexpressing the HPV16 oncogenes E6 and E7, as with the findings of RNA-seq. However, SOX2 and FYN expression levels were overexpressed, in contrast to RNA-seq results. The mRNA expression levels of CDH1, CDH2, EGF, IL-1 β , FGF2, BDNF, TLR4, IGF1, DLG4, COL1A1, CXCR4, and WNT5A were analyzed by RT-qPCR, and their expression was in agreement with the outcomes of RNA-Seq. (Figure 7 and Supplementary Figure 6).

Discussion

It is well known that E6 and E7 can attach to the ECM of the cervical squamous epithelium. Further, HPV E6 and E7 can be detected in a substantial proportion of women with cervical intraepithelial neoplasia (CIN) (Guan et al., 2012); they also serve as attractive targets for HPV-related diseases (Hoppe-Seyler et al., 2018). Owing to its specific sites and functions in antigen presentation, LCs are considered essential for the immune response against HPV infection (Cunningham et al., 2010). In the epidermis of mice (Kaplan et al., 2005) and female genital tract (Britto et al., 2020), LCs produce effector cytokines to stimulate T lymphocytes and B lymphocytes through interactions with C-type lectin (CLR receptors) and TLRs. Hubert et al. (Hubert et al., 2005) confirmed decreased levels

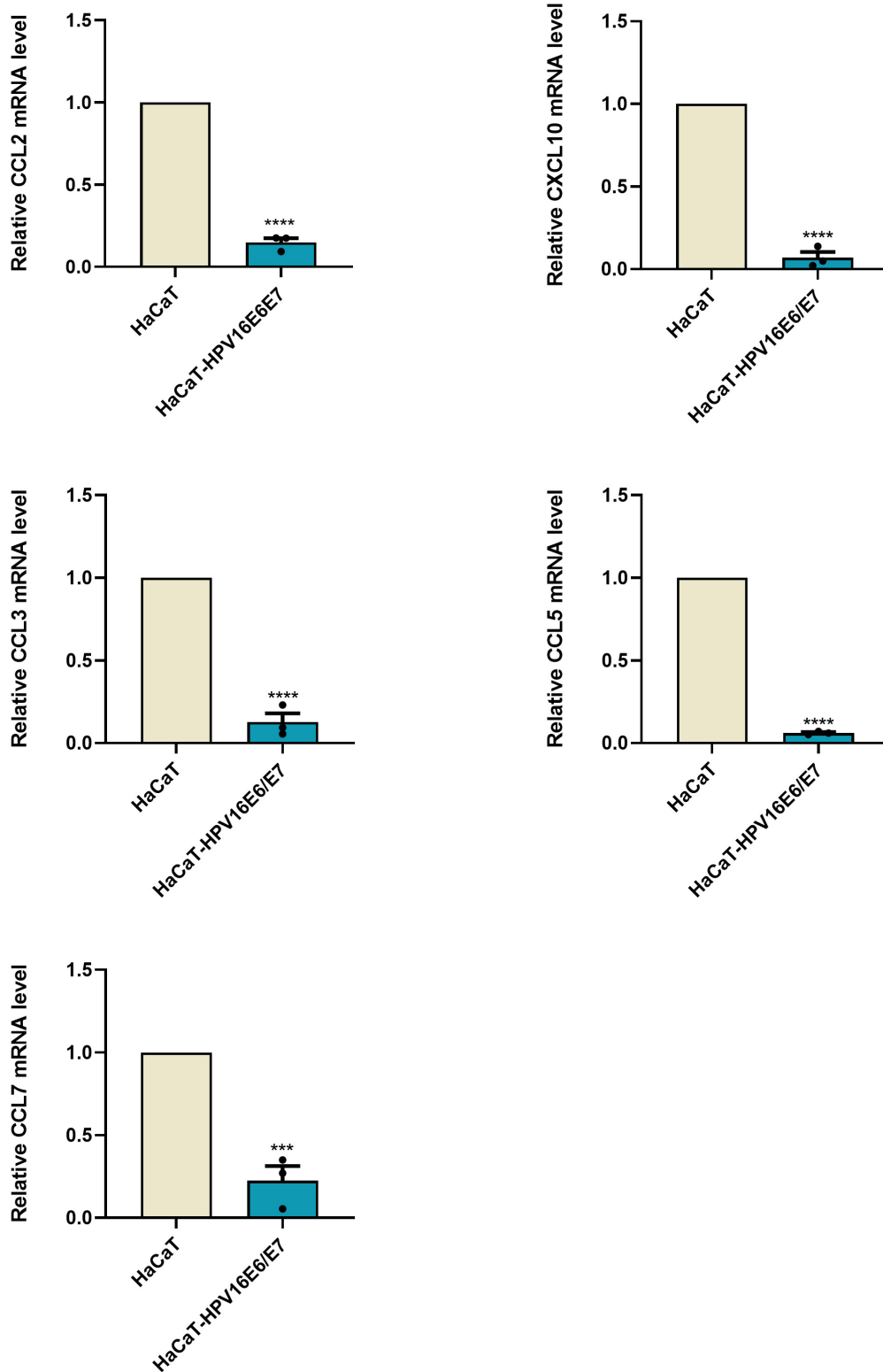
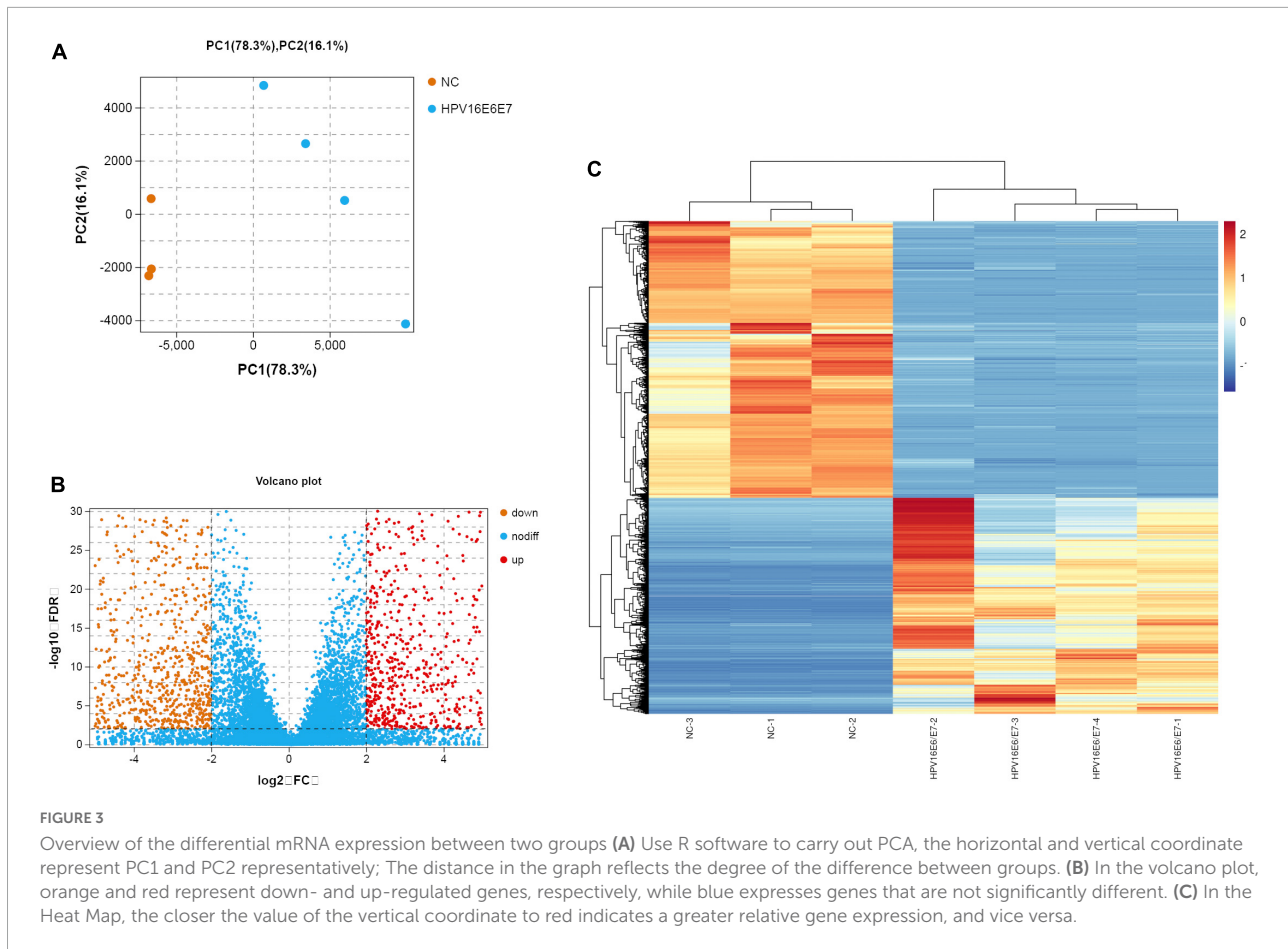


FIGURE 2

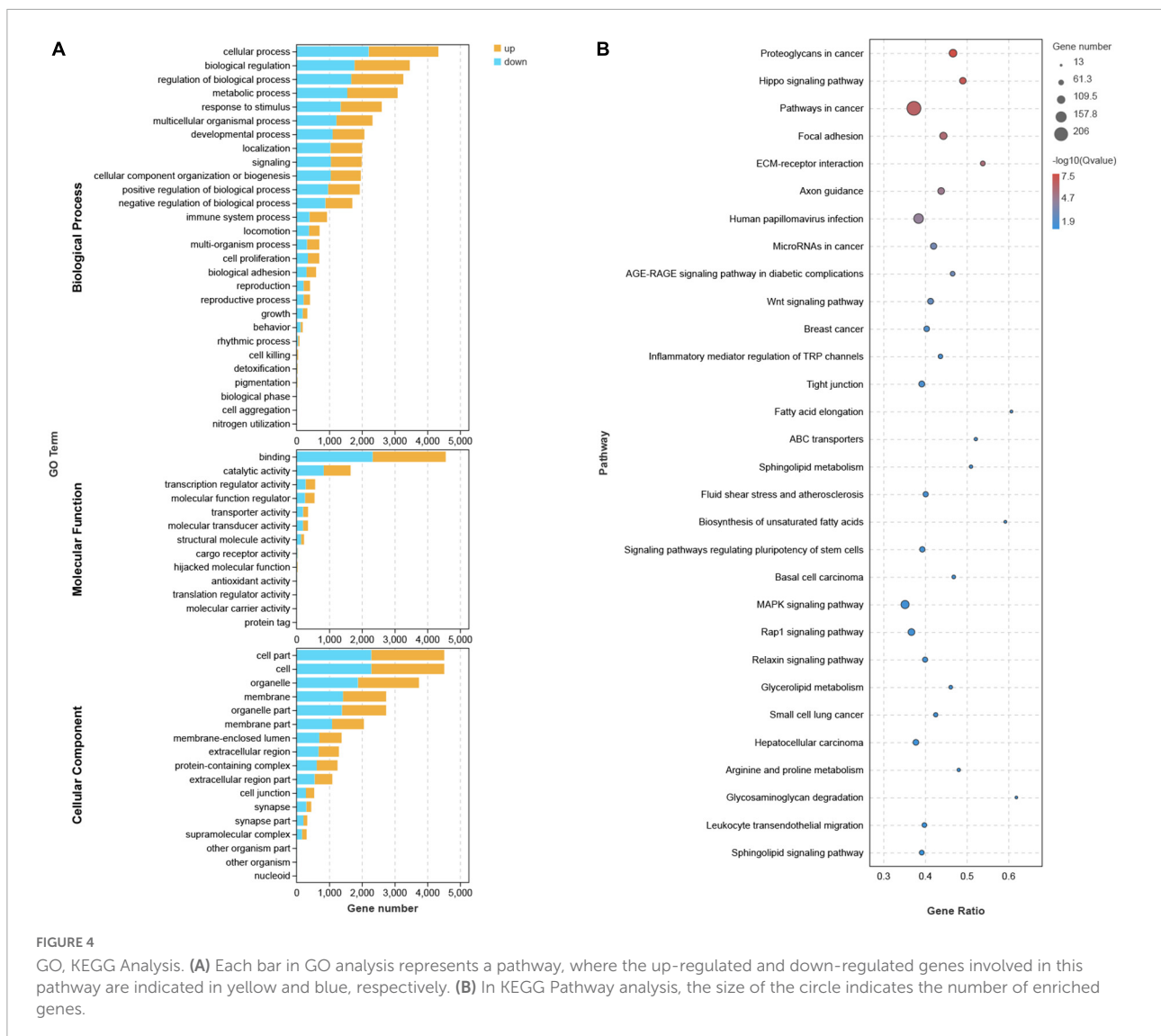
E6 and E7 damaged the secretion of chemokines in HaCaT RT-qPCR results were quantified by real-time PCR using GAPDH and β -ACTIN as internal control genes and presented in bar graph. It can be seen that overexpression of E6E7 does lead to a decrease in the relative expression of CCL2, CCL3, CCL5, CCL7, and CXCL10. *** $p < 0.001$, **** $p < 0.0001$.



of *CDH1* mRNA and numbers of $CD1\alpha^+$ LCs in squamous cell carcinoma and SILs compared with those in normal cervical epithelia. According to the high throughput screening of clinical specimens (Britto et al., 2020), the decrease observed in the mRNA levels of *CDH1*, *Claudin 1*, *Claudin 4*, and *ZO-1* mRNA and IFN signaling upon HPV infection indicate that it could result in weakness of the epithelial barrier (Aggarwal et al., 2019; Giorgi Rossi et al., 2021). Collectively, these findings suggest that the E6 and E7 oncoproteins are strongly associated with cell adhesion in HPV-induced immunosuppression. The loss of cell adhesion caused by the imbalance in adhesion molecules and chemokines might be another immune-escape strategy that has evolved in HPV.

CXC motif chemokine ligand 10 (CXCL10), CC motif chemokine ligand 2 (CCL2), CCL3, and CCL5 are pro-inflammatory chemokines that actively participate in the inflammatory response after viral exposure (Kolaczowska and Kubes, 2013). CCL2 (Nakamura et al., 1995; Kunstfeld et al., 1998; Hacke et al., 2010) is a key chemokine that attracts cells, including T lymphocytes, eosinophil granulocytes, macrophages, mast cells, and monocytes, to inflammatory sites. In general, CCL2 expression is activated after viral infection

and recruits Langerhans and DCs, respectively. However, co-expression of the E6 and E7 proteins inhibits CCL2 expression in primary epithelial cells of the female genital tract (Hacke et al., 2010). An *in vitro* study (Nakamura et al., 1995) has suggested that HPV E7 interacts with interferon regulatory factor 1 (IRF-1), a significant regulator of cellular immune responses, to suppress CCL2 expression. This partly explains the almost undetectable activation of potent anti-tumor immune responses in primary HPV-infected epithelial tissues. It has been reported that humans lack a robust inflammatory response against primary HPV infection and progressively lose immune cells in the cervical stroma during CIN (Kleine-Lowinski et al., 2003; Hacke et al., 2010; Garrido et al., 2021). CIN is strongly associated with CCL2 expression in the tumor microenvironment. Habbous et al. (2012) suggested that as CIN progresses, levels of many hosts immune response markers, including the chemokine CCL2, are reduced. However, the specific mechanisms involved remain unclear. As epithelial dysplasia progresses to cervical cancer, macrophages, T cells, and LCs of the cervical mucosa are depleted. Restoring CCL2 expression can specifically improve the anti-tumor immunity of the host and block disease progression. Therefore, exploring



the selective loss of CCL2 expression after E6/E7 transduction is crucial to blocking disease progression. However, in cell adhesion, the role of chemokines still needs to be explored in many ways. CXCL10 (Halle et al., 2017; Takeuchi and Saito, 2017) is associated with increased quantities of tumor-infiltrating CD8⁺ T cells, inducing the release of cytotoxic molecules (such as granzyme B and perforin) and apoptosis, which are associated with lower levels of cancer metastasis and improved patient survival in ovarian and colon cancer. CCL5 (Bruand et al., 2021) expression was found to be positively correlated with CD8⁺ T cell infiltration. T cell infiltration reportedly requires the secretion of CCL5 by cells in both epithelial cancer cell models and animal models. Zhang et al. (2020) suggested that CCL7 promotes anti-PD-1 therapy (CDC1) in a mouse model by recruiting conventional DCs to the tumor microenvironment to promote T cell proliferation. In addition, chemokines contribute to anti-tumor immunity by

recruiting tumor-associated antigen-presenting cells, promoting their binding to T cells, and influencing tumorigenesis by interacting with tumor stem cell-like cells and stromal cells (Kombe Kombe et al., 2020). In summary, different lymphocyte subsets are recruited into the tumor microenvironment through different chemokine–chemokine receptor signaling pathways. The restricted expression of chemokines directly or indirectly leads to the failure of anti-tumor immunity.

Our study revealed 1,644 upregulated mRNAs and 1,261 downregulated mRNAs after E6/E7 overexpression. According to RNA-seq analysis, there is a tight connection between DEGs and cell adhesion, focal adhesion, leukocyte–endothelial migration, tight junctions, and Hippo and Wnt signaling pathways. KEGG analysis revealed that these DEGs were highly focused in cancer proliferation-related pathways, including the MAPK, Hippo, Wnt, and cell adhesion signaling pathways. It has been suggested that E6/E7 might exhibit crosstalk

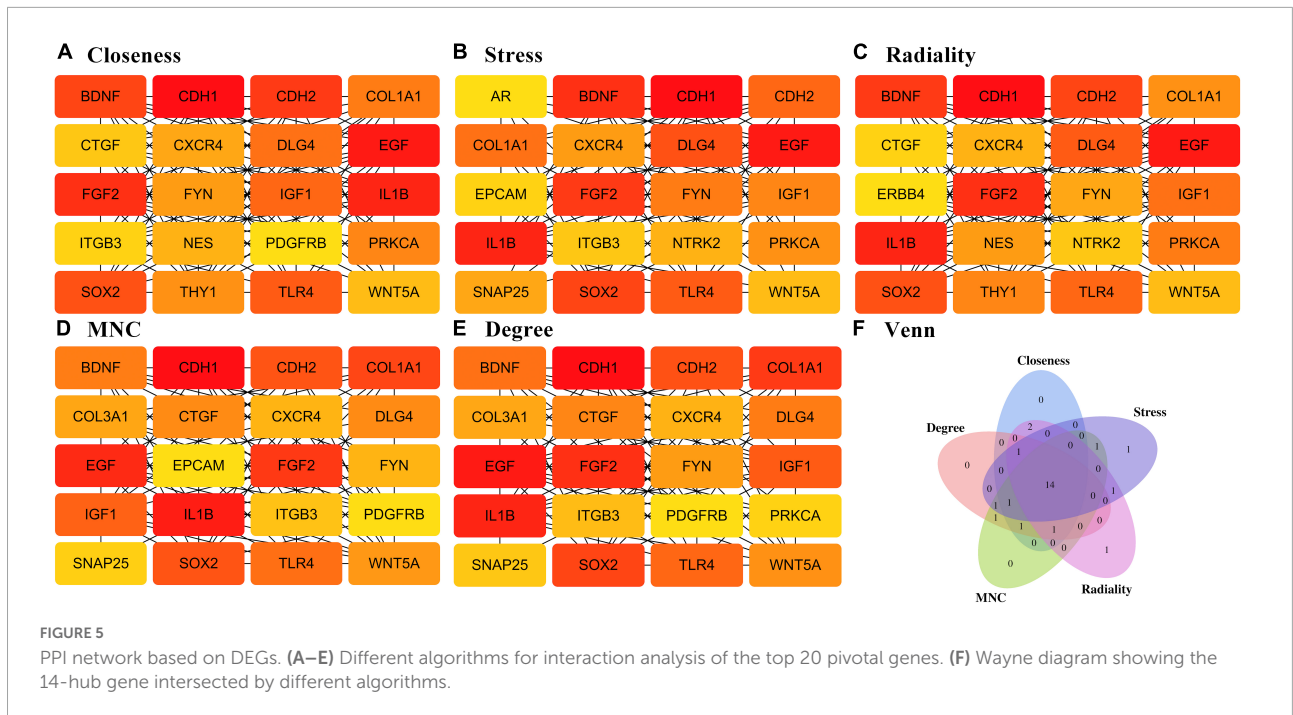


FIGURE 5 PPI network based on DEGs. (A–E) Different algorithms for interaction analysis of the top 20 pivotal genes. (F) Wayne diagram showing the 14-hub gene intersected by different algorithms.

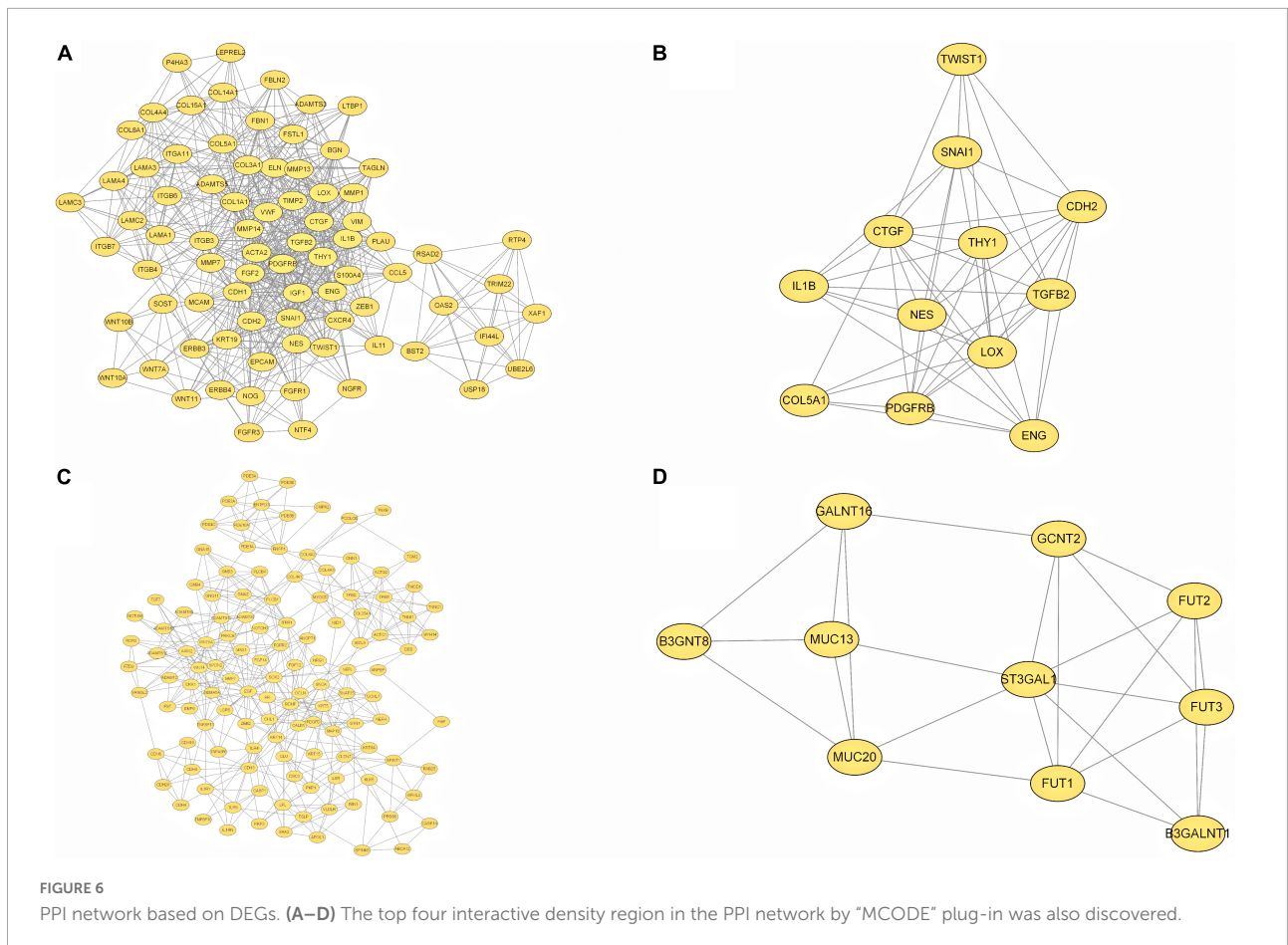


FIGURE 6 PPI network based on DEGs. (A–D) The top four interactive density region in the PPI network by “MCODE” plug-in was also discovered.

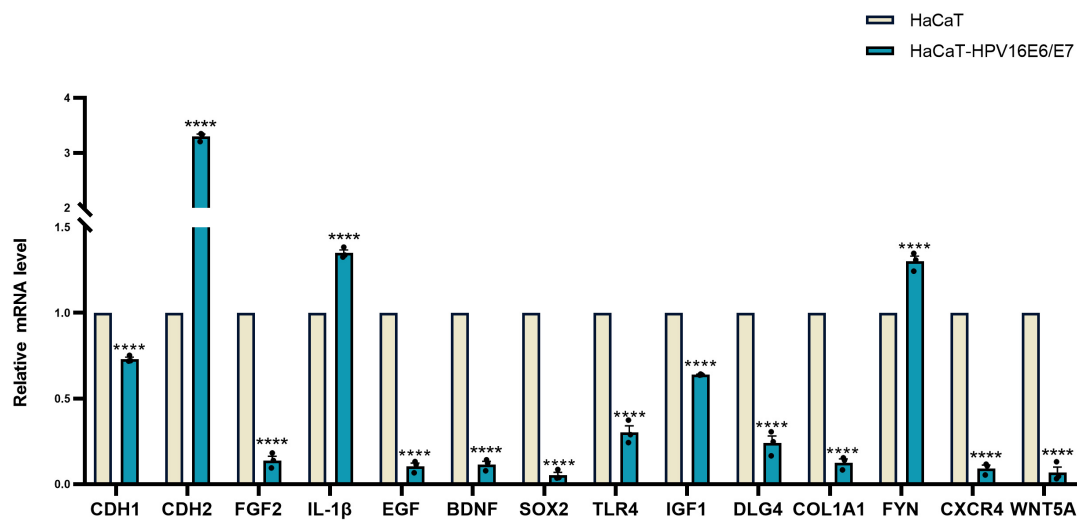


FIGURE 7

Verification of 14 hub gene Relative expression results of 14 hub gene were quantified by real-time PCR using GAPDH and β -ACTIN as internal control genes and shown by the bar graph whose horizontal and vertical coordinates represent the gene names and relative expressions, respectively. The verification is consistent with High-throughput sequencing results. **** $p < 0.0001$.

with these signaling pathways, affecting cell adhesion and limiting the immune response. CXCR4 (Zou et al., 1998; Goïta and Guenot, 2022) is a chemokine G protein-coupled transmembrane receptor released by stromal cells. Stromal cell-derived factor-1 (SDF-1; CXCL12), a ligand of CXCR4, induces B-cell proliferation and T-cell recruitment by activating CXCR4-expressing cells. Studies have demonstrated that the immune infiltration of B cells in the tumor microenvironment is associated with a survival advantage in patients with cervical (Abdul Rahman et al., 2020), breast (Hassel et al., 2021), and high-grade serous ovarian (Montfort et al., 2017) cancer; B cells are recruited through the binding of CXCL12 and CXCR4 (Greenbaum et al., 2013). Furthermore, CXCL12/CXCR4 enhances Src phosphorylation by activating MAPK or mitogen-activated protein kinase (MEK)/extracellular signal-regulated kinase (ERK) kinases (Kasina and Macoska, 2012). CXCR4-induced signaling cascades are commonly referred to as the “CXCR4–SDF-1 axis” and are frequently associated with lymphocyte trafficking and homing. To participate in the immune response (Peled et al., 1999), CXCL12 binds to CXCR4 to stimulate the firm adhesion of leukocytes by increasing integrin stability, which binds to intracellular adhesion molecules (ICAM-1) and vascular CAMs (VCAM-1). Researchers (Zheng et al., 2017) have used the CRISPR-Cas9 system in a cellular model to knock out CXCR4 and observed that colorectal cancer cell lines showed reduced adhesion to the ECM and endothelium, further demonstrating that CXCR4 is closely related to the Akt and type 1 insulin-like growth factor receptor (IGF1R) signaling pathways. In mouse models (Aggarwal et al., 2019), the CXCL12/CXCR4 axis enhances the function of M1-type macrophages, stimulates the production

of inflammatory cytokines, and increases the phagocytosis of pathogens. Furthermore, it has been shown that CXCL12 primes IL-1 production in M2 macrophages by inducing its receptor CXCR4 and directly mediating the activation of CD4⁺T cells (Yu et al., 2020). Macrophages, an essential component of the innate immune system, are highly heterogeneous and malleable, and the reduced expression of CXCR4 might affect the dysregulation of M1/M2 phenotypes (Beneduce et al., 2019). This could play a vital role in the immune escape mediated by E6 and E7. These results suggest that CXCL12/CXCR4 is a potential therapeutic target for treating autoimmune diseases, including human immunodeficiency virus infection, cancer, warts, and immunodeficiency (Comba et al., 2020).

The expression of E6 and E7 resulted in the detection of many DEGs using RNA-seq and RT-qPCR. Fourteen of these hub genes were linked to cell adhesion (Chute, 2006; Teicher and Fricker, 2010; Paolillo and Schinelli, 2019; Marotta et al., 2021), leukocyte–endothelial migration (Yakovlev et al., 2019; Morein et al., 2020; Yan et al., 2021), stem cell signaling (Davidson et al., 2007; Bijlmakers, 2009), and epithelial–mesenchymal transition (Pastushenko et al., 2021; Wang et al., 2021). Based on these experimental and bioinformatics analyses, we hypothesized that HPV16 E6 and E7 signaling causes differential mRNA expression through direct or indirect mRNA pathways that regulate cell adhesion and chemokine secretion.

In this study, we used RNA-seq, RT-qPCR, and bioinformatics to validate the HPV-associated signaling pathways and possible downstream signaling molecules of the E6 and E7 proteins in human keratinocytes. This study

provides a new direction and basis for further elucidation of the mechanism of E6/E7-mediated cell adhesion suppression. However, on the one hand, our study was restricted to *in vitro* conditions and the mode of interaction between CCL2 and hub genes is unclear in keratinocytes immortalized with both HPV E6 and E7 genes. The detailed mechanism will be investigated profoundly in our future studies. On the other hand, although some studies have indicated that FGF stimulation produces phosphorylation of E-cadherin and β -catenin on tyrosine residues, as well as increased E-cadherin localization to the cytoplasmic membrane and association with FGFR1 demonstrable by co-immunoprecipitation in the human pancreatic adenocarcinoma cell lines (BxPc3, T3M4 and HPAF), more direct interactions between hub genes need to be verified by co-immunoprecipitation or immunoblastic hybridization in our cellular models. The levels of mRNA only respond to the transcriptional aspect, while the process of post-translational modifications is highly variable, with different modifications resulting in different protein expression. Such differences may be influenced by post-transcriptional mechanisms such as methylation and acetylation. A previous study revealed that the level of m6A-modified mRNA is increased in cancer cells during the epithelial-mesenchymal transition of hepatocellular carcinoma cell metastasis (Lin et al., 2019). Although several studies have confirmed that the mRNA levels of certain hub genes such as CHD1, CDH2 (Castillo et al., 2016; Wang et al., 2020), IL-1 β , EGF (Fu et al., 2020), BDNF (McDole et al., 2015), SOX2 (Scapin et al., 2019), and TLR4 (Jin et al., 2017) were consistent with the protein levels, it has not been validated in HaCaT-HPV16E6E7 cells. Considering this special feature, we will focus on discovering and exploring the differences in hub gene at the mRNA and protein levels in our future studies. It is undeniable that lentiviral vectors have an effect on gene expression, and we chose parental HaCaT as a negative control in our study, which makes it difficult to exclude the differential gene changes that would result from null loading at this time.

Data availability statement

The data presented in this study are deposited in the SRA repository, accession number: PRJNA850539 can be found in the article/[Supplementary material](#).

Author contributions

RD and QR conceived and designed the experiments and revised the manuscript. RD and XL performed the experiments. RT carried out RNA-seq. RD, RT, SZ, TS, and QR analyzed

the data. RD wrote the manuscript. All authors have read and approved the final manuscript.

Funding

This work was supported by the National Natural Science Foundation of China (General Program, 8207150903), the Chinese Clinical Medicine Innovation Center of Obstetrics, Gynecology, and Reproduction in Jiangsu Province (ZX202102), and the Postgraduate Research and Practice Innovation Program of Jiangsu Province, China (KYCX21_1680).

Acknowledgments

We thank Micaella Aliza from Editage for editing the manuscript.

Conflict of interest

The authors declare that the research was conducted in the absence of any commercial or financial relationships that could be construed as a potential conflict of interest.

Publisher's note

All claims expressed in this article are solely those of the authors and do not necessarily represent those of their affiliated organizations, or those of the publisher, the editors and the reviewers. Any product that may be evaluated in this article, or claim that may be made by its manufacturer, is not guaranteed or endorsed by the publisher.

Supplementary material

The Supplementary Material for this article can be found online at: <https://www.frontiersin.org/articles/10.3389/fmicb.2022.979087/full#supplementary-material>

SUPPLEMENTARY FIGURE 1

Verification of HPV 16 E6/E7 Stable Expression HaCaT Cell Line Clone#4, #6, #10, #11 The results suggested that HPV 16 E6/E7 Stable Expression HaCaT Cell Line Clone#4, #6, #10, #11 all displayed significant overexpression of HPV16 E6 and E7. While, Clone#11 showed the highest expression of target gene, validated by RT-qPCR method.

SUPPLEMENTARY FIGURE 2

The original western blots of HPV16E6 with protein markers WB results showed that the expression of β -actin as an internal reference HPV16 E6 was reduced in protein level.

SUPPLEMENTARY FIGURE 3

The original western blots of HPV16E7 with protein markers WB results showed that the expression of β -actin as an internal reference HPV16 E7 was reduced in protein level.

SUPPLEMENTARY FIGURE 4

(A) RT-qPCR results that used β -ACTIN as internal control genes. **(B)** RT-qPCR results that used GAPDH as internal control genes. Verification of 14 hub gene RT-qPCR results were quantified by real-time PCR using GAPDH and β -ACTIN as internal control genes, respectively. It can be seen in bar graph that the verification is consistent with the results of **Figure 1**. *** $p < 0.001$, **** $p < 0.0001$.

SUPPLEMENTARY FIGURE 5

GESAs analyses The vertical coordinate is the ES value and the horizontal coordinate is the sequencing of the gene. According to the result of gene sequencing, the genes in that pathway/term are scored plus and the genes not in that pathway/term are scored minus. The final

maximum value obtained is the maximum value for that pathway/term. The points that are added will be marked with "vertical lines" below the graph.

SUPPLEMENTARY FIGURE 6

Verification of 14 hub gene Relative expression results of 14 hub gene were quantified by real-time PCR using GAPDH and β -ACTIN as internal control genes, respectively and shown by the bar graph whose horizontal and vertical coordinates represent the gene, names and relative expressions, respectively. The verification is consistent with the results of **Figure 7**. * $p < 0.05$, ** $p < 0.01$, *** $p < 0.001$, and **** $p < 0.0001$.

SUPPLEMENTARY MATERIAL

The differential expression analysis results (DESeq2_analysis_results) used in this study were uploaded, and these tables were placed in the Supplementary Material.

References

- Abdul Rahman, S. F., Xiang Lian, B. S., and Mohana-Kumaran, N. (2020). Targeting the B-cell lymphoma 2 anti-apoptotic proteins for cervical cancer treatment. *Future Oncol.* 16, 2235–2249. doi: 10.2217/fon-2020-0389
- Acevedo-Sánchez, V., Rodríguez-Hernández, R. M., Aguilar-Ruiz, S. R., Torres-Aguilar, H., and Romero-Tlalolini, M. L. A. (2021). Extracellular vesicles in cervical cancer and HPV infection. *Membranes (Basel)* 11:453. doi: 10.3390/membranes11060453
- Aggarwal, C., Cohen, R. B., Morrow, M. P., Kravnyak, K. A., Sylvester, A. J., Knoblock, D. M., et al. (2019). Immunotherapy targeting HPV16/18 generates potent immune responses in HPV-associated head and neck cancer. *Clin. Cancer Res.* 25, 110–124. doi: 10.1158/1078-0432.Ccr-18-1763
- Attademo, L., Tuninetti, V., Pisano, C., Cecere, S. C., Di Napoli, M., Tambaro, R., et al. (2020). Immunotherapy in cervix cancer. *Cancer Treat Rev.* 90:102088. doi: 10.1016/j.ctrv.2020.102088
- Beneduce, E., Matte, A., De Falco, L., Mbiandjeu, S., Chiabrando, D., Tolosano, E., et al. (2019). Fyn kinase is a novel modulator of erythropoietin signaling and stress erythropoiesis. *Am. J. Hematol.* 94, 10–20. doi: 10.1002/ajh.25295
- Bijlmakers, M. J. (2009). Protein acylation and localization in T cell signaling (Review). *Mol. Membr. Biol.* 26, 93–103. doi: 10.1080/09687680802650481
- Britto, A. M. A., Goes, L. R., Sívro, A., Policarpo, C., Meirelles, ÂR., Furtado, Y., et al. (2020). HPV Induces changes in innate immune and adhesion molecule markers in cervical mucosa with potential impact on HIV infection. *Front. Immunol.* 11:2078. doi: 10.3389/fimmu.2020.02078
- Bruand, M., Barras, D., Mina, M., Ghisoni, E., Morotti, M., Lanitis, E., et al. (2021). Cell-autonomous inflammation of BRCA1-deficient ovarian cancers drives both tumor-intrinsic immunoreactivity and immune resistance via STING. *Cell Rep.* 36:109412. doi: 10.1016/j.celrep.2021.109412
- Bule, P., Aguiar, S. I., Aires-Da-Silva, F., and Dias, J. N. R. (2021). Chemokine-directed tumor microenvironment modulation in cancer immunotherapy. *Int. J. Mol. Sci.* 22:9804. doi: 10.3390/ijms22189804
- Castillo, L. F., Tascón, R., Lago Huvelles, M. R., Novack, G., Llorens, M. C., Dos Santos, A. F., et al. (2016). Glypican-3 induces a mesenchymal to epithelial transition in human breast cancer cells. *Oncotarget* 7, 60133–60154. doi: 10.18632/oncotarget.11107
- Chute, J. P. (2006). Stem cell homing. *Curr. Opin. Hematol.* 13, 399–406. doi: 10.1097/01.moh.0000245698.62511.3d
- Comba, A., Dunn, P. J., Argento, A. E., Kadiyala, P., Ventosa, M., Patel, P., et al. (2020). Fyn tyrosine kinase, a downstream target of receptor tyrosine kinases, modulates anti-glioma immune responses. *Neuro Oncol.* 22, 806–818. doi: 10.1093/neuonc/noaa006
- Cunningham, A. L., Abendroth, A., Jones, C., Nasr, N., and Turville, S. (2010). Viruses and langerhans cells. *Immunol. Cell Biol.* 88, 416–423. doi: 10.1038/icb.2010.42
- Davidson, D., Schraven, B., and Veillette, A. (2007). PAG-associated FynT regulates calcium signaling and promotes energy in T lymphocytes. *Mol. Cell Biol.* 27, 1960–1973. doi: 10.1128/mcb.01983-06
- Dunne, E. F., and Park, I. U. (2013). HPV and HPV-associated diseases. *Infect. Dis. Clin. North Am.* 27, 765–778. doi: 10.1016/j.idc.2013.09.001
- Dustin, M. L. (2009). Supported bilayers at the vanguard of immune cell activation studies. *J. Struct. Biol.* 168, 152–160. doi: 10.1016/j.jsb.2009.05.007
- Ferragut, F., Vachetta, V. S., Troncoso, M. F., Rabinovich, G. A., and Elola, M. T. (2021). ALCAM/CD166: A pleiotropic mediator of cell adhesion, stemness and cancer progression. *Cytokine Growth Factor Rev.* 61, 27–37. doi: 10.1016/j.cytogfr.2021.07.001
- Fu, B., Yin, S., Lin, X., Shi, L., Wang, Y., Zhang, S., et al. (2020). PTPN14 aggravates inflammation through promoting proteasomal degradation of SOCS7 in acute liver failure. *Cell Death Dis.* 11:803. doi: 10.1038/s41419-020-03014-7
- Garrido, F., Wild, C. M., Mittelberger, J., Dobler, F., Schneider, M., Ansoorge, N., et al. (2021). The role of chemokines in cervical cancers. *Medicina (Kaunas)* 57:1141. doi: 10.3390/medicina57111141
- Giorgi Rossi, P., Carozzi, F., Ronco, G., Allia, E., Bisanzio, S., Gillio-Tos, A., et al. (2021). p16/ki67 and E6/E7 mRNA accuracy and prognostic value in triaging HPV DNA-positive women. *J. Natl. Cancer Inst.* 113, 292–300. doi: 10.1093/jnci/djaa105
- Goïta, A. A., and Guenot, D. (2022). Colorectal cancer: The contribution of CXCL12 and its receptors CXCR4 and CXCR7. *Cancers (Basel)* 14:1810. doi: 10.3390/cancers14071810
- Greenbaum, A., Hsu, Y. M., Day, R. B., Schuettel, L. G., Christopher, M. J., Borgerding, J. N., et al. (2013). CXCL12 in early mesenchymal progenitors is required for haematopoietic stem-cell maintenance. *Nature* 495, 227–230. doi: 10.1038/nature11926
- Guan, P., Howell-Jones, R., Li, N., Bruni, L., de Sanjosé, S., Franceschi, S., et al. (2012). Human papillomavirus types in 115,789 HPV-positive women: A meta-analysis from cervical infection to cancer. *Int. J. Cancer* 131, 2349–2359. doi: 10.1002/ijc.27485
- Habbous, S., Pang, V., Eng, L., Xu, W., Kurtz, G., Liu, F. F., et al. (2012). p53 Arg72Pro polymorphism. HPV status and initiation, progression, and development of cervical cancer: A systematic review and meta-analysis. *Clin. Cancer Res.* 18, 6407–6415. doi: 10.1158/1078-0432.Ccr-12-1983
- Hacke, K., Rincon-Orozco, B., Buchwalter, G., Siehler, S. Y., Wasylyk, B., Wiesmüller, L., et al. (2010). Regulation of MCP-1 chemokine transcription by p53. *Mol. Cancer* 9:82. doi: 10.1186/1476-4598-9-82
- Halle, S., Halle, O., and Förster, R. (2017). Mechanisms and dynamics of T cell-mediated cytotoxicity in vivo. *Trends Immunol.* 38, 432–443. doi: 10.1016/j.it.2017.04.002
- Hassel, C., Gausserès, B., Guzylack-Piriou, L., and Foucras, G. (2021). Ductal macrophages predominate in the immune landscape of the lactating mammary gland. *Front. Immunol.* 12:754661. doi: 10.3389/fimmu.2021.754661
- Honig, B., and Shapiro, L. (2020). Adhesion protein structure. Molecular affinities, and principles of cell-cell recognition. *Cell* 181, 520–535. doi: 10.1016/j.cell.2020.04.010
- Hoppe-Seyler, K., Bossler, F., Braun, J. A., Herrmann, A. L., and Hoppe-Seyler, F. (2018). The HPV E6/E7 oncogenes: Key Factors for viral carcinogenesis and therapeutic targets. *Trends Microbiol.* 26, 158–168. doi: 10.1016/j.tim.2017.07.007

- Howie, H. L., Katzenellenbogen, R. A., and Galloway, D. A. (2009). Papillomavirus E6 proteins. *Virology* 384, 324–334. doi: 10.1016/j.virol.2008.11.017
- Hubert, P., Caberg, J. H., Gilles, C., Bousarghin, L., Franzen-Detrooz, E., Boniver, J., et al. (2005). E-cadherin-dependent adhesion of dendritic and Langerhans cells to keratinocytes is defective in cervical human papillomavirus-associated (pre)neoplastic lesions. *J. Pathol.* 206, 346–355. doi: 10.1002/path.1771
- Janiszewska, M., Primi, M. C., and Izard, T. (2020). Cell adhesion in cancer: Beyond the migration of single cells. *J. Biol. Chem.* 295, 2495–2505. doi: 10.1074/jbc.REV119.007759
- Jin, X., Chen, C., Li, D., Su, Q., Hang, Y., Zhang, P., et al. (2017). PRDX2 in myocyte hypertrophy and survival is mediated by TLR4 in acute infarcted myocardium. *Sci. Rep.* 7:6970. doi: 10.1038/s41598-017-06718-7
- Kaplan, D. H., Jenison, M. C., Saeland, S., Shlomchik, W. D., and Shlomchik, M. J. (2005). Epidermal langerhans cell-deficient mice develop enhanced contact hypersensitivity. *Immunity* 23, 611–620. doi: 10.1016/j.immuni.2005.10.008
- Kasina, S., and Macoska, J. A. (2012). The CXCL12/CXCR4 axis promotes ligand-independent activation of the androgen receptor. *Mol. Cell. Endocrinol.* 351, 249–263. doi: 10.1016/j.mce.2011.12.015
- Kleine-Lowinski, K., Rheinwald, J. G., Fichorova, R. N., Anderson, D. J., Basile, J., Münger, K., et al. (2003). Selective suppression of monocyte chemoattractant protein-1 expression by human papillomavirus E6 and E7 oncoproteins in human cervical epithelial and epidermal cells. *Int. J. Cancer* 107, 407–415. doi: 10.1002/ijc.11411
- Kolaczowska, E., and Kubes, P. (2013). Neutrophil recruitment and function in health and inflammation. *Nat. Rev. Immunol.* 13, 159–175. doi: 10.1038/nri3399
- Kombe Kombe, A. J., Li, B., Zahid, A., Mengist, H. M., Bounda, G. A., Zhou, Y., et al. (2020). Epidemiology and Burden of human papillomavirus and related diseases, molecular pathogenesis, and vaccine evaluation. *Front. Public Health* 8:552028. doi: 10.3389/fpubh.2020.552028
- Kunstfeld, R., Lechleitner, S., Wolff, K., and Petzelbauer, P. (1998). MCP-1 and MIP-1 α are most efficient in recruiting T cells into the skin in vivo. *J. Invest. Dermatol.* 111, 1040–1044. doi: 10.1046/j.1523-1747.1998.00410.x
- Läubli, H., and Borsig, L. (2019). Altered cell adhesion and glycosylation promote cancer immune suppression and metastasis. *Front. Immunol.* 10:2120. doi: 10.3389/fimmu.2019.02120
- Lin, X., Chai, G., Wu, Y., Li, J., Chen, F., Liu, J., et al. (2019). RNA m(6A) methylation regulates the epithelial mesenchymal transition of cancer cells and translation of Snail. *Nat. Commun.* 10:2065. doi: 10.1038/s41467-019-09865-9
- Login, F. H., Jensen, H. H., Pedersen, G. A., Koffman, J. S., Kwon, T. H., Parsons, M., et al. (2019). Aquaporins differentially regulate cell-cell adhesion in MDCK cells. *FASEB J.* 33, 6980–6994. doi: 10.1096/fj.201802068RR
- Marotta, G., Basagni, F., Rosini, M., and Minarini, A. (2021). Role of fyn kinase inhibitors in switching neuroinflammatory pathways. *Curr. Med. Chem.* 29, 4738–4755. doi: 10.2174/0929867329666211221153719
- McDole, B., Isgor, C., Pare, C., and Guthrie, K. (2015). BDNF over-expression increases olfactory bulb granule cell dendritic spine density in vivo. *Neuroscience* 304, 146–160. doi: 10.1016/j.neuroscience.2015.07.056
- Montfort, A., Pearce, O., Maniati, E., Vincent, B. G., Bixby, L., Böhm, S., et al. (2017). A strong B-cell response is part of the immune landscape in human high-grade serous ovarian metastases. *Clin. Cancer Res.* 23, 250–262. doi: 10.1158/1078-0432.Ccr-16-0081
- Morein, D., Erlichman, N., and Ben-Baruch, A. (2020). Beyond cell motility: The expanding roles of chemokines and their receptors in malignancy. *Front. Immunol.* 11:952. doi: 10.3389/fimmu.2020.00952
- Nakamura, K., Williams, I. R., and Kupper, T. S. (1995). Keratinocyte-derived monocyte chemoattractant protein 1 (MCP-1): Analysis in a transgenic model demonstrates MCP-1 can recruit dendritic and Langerhans cells to skin. *J. Invest. Dermatol.* 105, 635–643. doi: 10.1111/1523-1747.ep12324061
- Oldak, M., Smola-Hess, S., and Maksym, R. (2006). Integrin beta4, keratinocytes and papillomavirus infection. *Int. J. Mol. Med.* 17, 195–202.
- Paolillo, M., and Schinelli, S. (2019). Extracellular matrix alterations in metastatic processes. *Int. J. Mol. Sci.* 20:4947. doi: 10.3390/ijms20194947
- Pastushenko, I., Mauri, F., Song, Y., de Cock, F., Meeusen, B., Swedlund, B., et al. (2021). Fat1 deletion promotes hybrid EMT state, tumour stemness and metastasis. *Nature* 589, 448–455. doi: 10.1038/s41586-020-03046-1
- Peled, A., Grabovsky, V., Habler, L., Sandbank, J., Arenzana-Seisdedos, F., Petit, I., et al. (1999). The chemokine SDF-1 stimulates integrin-mediated arrest of CD34(+) cells on vascular endothelium under shear flow. *J. Clin. Invest.* 104, 1199–1211. doi: 10.1172/jci7615
- Scapin, C., Ferri, C., Pettinato, E., Zamboni, D., Bianchi, F., Del Carro, U., et al. (2019). Enhanced axonal neuregulin-1 type-III signaling ameliorates neurophysiology and hypomyelination in a Charcot-Marie-Tooth type 1B mouse model. *Hum. Mol. Genet.* 28, 992–1006. doi: 10.1093/hmg/ddy411
- Schiffman, M., Castle, P. E., Jeronimo, J., Rodriguez, A. C., and Wacholder, S. (2007). Human papillomavirus and cervical cancer. *Lancet* 370, 890–907. doi: 10.1016/s0140-6736(07)61416-0
- Schimmel, L., and Gordon, E. (2018). The precise molecular signals that control endothelial cell-cell adhesion within the vessel wall. *Biochem. Soc. Trans.* 46, 1673–1680. doi: 10.1042/bst20180377
- Sumigray, K. D., and Lechler, T. (2015). Cell adhesion in epidermal development and barrier formation. *Curr. Top. Dev. Biol.* 112, 383–414. doi: 10.1016/bs.ctdb.2014.11.027
- Takeuchi, A., and Saito, T. (2017). CD4 CTL, a Cytotoxic Subset of CD4(+) T Cells, Their differentiation and function. *Front. Immunol.* 8:194. doi: 10.3389/fimmu.2017.00194
- Tao, R., Huang, F., Lin, K., Lin, S. W., Wei, D. E., and Luo, D. S. (2021). Using RNA-Seq to explore the hub genes in the trigeminal root entry zone of rats by compression injury. *Pain Physician* 24, E573–E581.
- Te Riet, J., Helenius, J., Strohmeyer, N., Cambi, A., Figdor, C. G., and Müller, D. J. (2014). Dynamic coupling of ALCAM to the actin cortex strengthens cell adhesion to CD6. *J. Cell Sci.* 127(Pt 7), 1595–1606. doi: 10.1242/jcs.141077
- Teicher, B. A., and Fricker, S. P. (2010). CXCL12 (SDF-1)/CXCR4 pathway in cancer. *Clin. Cancer Res.* 16, 2927–2931. doi: 10.1158/1078-0432.Ccr-09-2329
- von Lersner, A., Drogen, L., and Zijlstra, A. (2019). Modulation of cell adhesion and migration through regulation of the immunoglobulin superfamily member ALCAM/CD166. *Clin. Exp. Metastasis* 36, 87–95. doi: 10.1007/s10585-019-09957-2
- Wang, F., Tao, R., Zhao, L., Hao, X. H., Zou, Y., Lin, Q., et al. (2021). Differential lncRNA/mRNA Expression profiling and functional network analyses in Bmp2 deletion of mouse dental papilla cells. *Front. Genet.* 12:702540. doi: 10.3389/fgene.2021.702540
- Wang, H., Wang, Z., Li, Y., Lu, T., and Hu, G. (2020). Silencing snail reverses epithelial-mesenchymal transition and increases radiosensitivity in hypopharyngeal carcinoma. *Oncol. Targets Ther.* 13, 497–511. doi: 10.2147/ott.S237410
- Whiteside, M. A., Siegel, E. M., and Unger, E. R. (2008). Human papillomavirus and molecular considerations for cancer risk. *Cancer* 113(10 Suppl), 2981–2994. doi: 10.1002/cncr.23750
- Yakovlev, S., Cao, C., Galisteo, R., Zhang, L., Strickland, D. K., and Medved, L. (2019). Fibrin-VLDL Receptor-dependent pathway promotes leukocyte transmigration by inhibiting Src kinase fyn and is a target for fibrin β 15-42 peptide. *Thromb. Haemost.* 119, 1816–1826. doi: 10.1055/s-0039-1695008
- Yan, S. L., Hwang, I. Y., Kamenyeva, O., Kabat, J., Kim, J. S., Park, C., et al. (2021). Unrestrained $G\alpha(i2)$ Signaling disrupts neutrophil trafficking, aging, and clearance. *Front. Immunol.* 12:679856. doi: 10.3389/fimmu.2021.679856
- Yu, J., Zhou, Z., Wei, Z., Wu, J., OuYang, J., Huang, W., et al. (2020). FYN promotes gastric cancer metastasis by activating STAT3-mediated epithelial-mesenchymal transition. *Transl. Oncol.* 13:100841. doi: 10.1016/j.tranon.2020.100841
- Zhang, M., Yang, W., Wang, P., Deng, Y., Dong, Y. T., Liu, F. F., et al. (2020). CCL7 recruits cDC1 to promote antitumor immunity and facilitate checkpoint immunotherapy to non-small cell lung cancer. *Nat. Commun.* 11:6119. doi: 10.1038/s41467-020-19973-6
- Zheng, F., Zhang, Z., Flamini, V., Jiang, W. G., and Cui, Y. (2017). The axis of CXCR4/SDF-1 Plays a role in colon cancer cell adhesion through regulation of the AKT and IGF1R signalling pathways. *Anticancer Res.* 37, 4361–4369. doi: 10.21873/anticancer.11830
- Zhu, S., Li, Y., Bennett, S., Chen, J., Weng, I. Z., Huang, L., et al. (2020). The role of glial cell line-derived neurotrophic factor family member artemin in neurological disorders and cancers. *Cell Prolif.* 53:e12860. doi: 10.1111/cpr.12860
- Zou, Y. R., Kottmann, A. H., Kuroda, M., Taniuchi, I., and Littman, D. R. (1998). Function of the chemokine receptor CXCR4 in hematopoiesis and in cerebellar development. *Nature* 393, 595–599. doi: 10.1038/31269